ELSEVIER

Materials Science and Engineering A352 (2003) 55–63

MATERIALS SCIENCE & ENGINEERING A

www.elsevier.com/locate/msea

Acoustic emission study on WC–Co thermal sprayed coatings

J.M. Miguel [a], J.M. Guilemany [a,*], B.G. Mellor [b], Y.M. Xu [b]

[a] CPT (Thermal Spray Centre), Materials Engineering, Dept. d'Enginyeria Química i Metal.lúrgia, Universitat de Barcelona, E-08028 Barcelona, Spain
[b] Materials Research Group, School of Engineering Sciences, University of Southampton, Southampton SO17 1BJ, UK

Received 21 November 2001; received in revised form 18 July 2002

Abstract

Thermally sprayed coatings contain residual stresses that are produced in the spraying process. These may reduce the coating lifetime. In order to determine the optimum spraying conditions with respect to the residual stress level present, the acoustic emission (AE) during four-point bend tests on tungsten carbide–cobalt coatings sprayed onto mild steel substrates was investigated. Samples tested at different levels of deformation were studied by means of scanning electron microscopy and AE in order to understand the cracking mechanisms. Relationships between the number and amplitude of AE events detected and the type of cracking processes occurring were established. It has been possible to compare the residual stresses caused by the effect of different spraying parameters, such as coating thickness, spraying distance and high velocity oxy-fuel gun.

Keywords: WC–Co; Acoustic emission; Bending test; Fracture mechanism

1. Introduction

Thermal spraying is a coating technique widely used to modify the surface properties of a substrate. A wide range of materials, such as ceramics, cermets, pure metals or alloys and polymeric materials can be deposited by this technique. Applications include protection from wear, high temperatures, corrosive agents, and more mundane uses in environmental corrosion protection in infrastructure maintenance engineering. The principle of thermal spray is to melt material feedstock (wire or powder), to accelerate the melt to impact on a substrate where rapid solidification and deposit build-up occurs [1]. Among the diverse spray processes available, high velocity oxy-fuel spraying (HVOF) is one of the most used because coatings with a high density, superior bond strength and with less degradation than that obtained with many other thermal spray processes are achieved. Excellent coating properties are produced by the high particle velocity, 400–800 m s^{-1}, realised [2] and from the low flame temperature of 2800–3200 K. These spraying parameters depend on the working gases, gas flow rates and gun geometry [3]. Considerable development has taken place in spraying gun design over recent years leading to guns being classified as first, second and third generation. Third generation guns, e.g. the DJ 2700 gun, have a greater gas pressure in the combustion chamber than second-generation guns, e.g. the CDS 100 gun, which means that the gas velocity and thus the velocity of particles leaving the gun are greater. This reduces the residence time of particles in the flame. However, as the temperature of the gases is similar for both guns the amount of thermal degradation of the particles is reduced for third generation guns.

Tungsten carbide–cobalt (WC–Co) cermets are used to produce materials with a wide range of physical and mechanical properties by combining the hard, brittle WC phase and the ductile cobalt phase in different proportions. During thermal spraying WC–Co particles are degraded and new phases are formed because of the loss of carbon by oxidation and reaction of the W with the metallic phase present. The new phases have been identified as W_2C, $CoWO_4$, $Co_xW_yC_z$, and metallic W [4]. The wear properties of WC–Co coatings are excellent and they are widely used to produce protective coatings on surfaces where abrasion, erosion and other

* Corresponding author. Tel.: +34-934021302; fax: +34-934021638.
E-mail address: cpt@material.qui.ub.es (J.M. Guilemany).

0921-5093/02/$ - see front matter
doi:10.1016/S0921-5093(02)00546-4

forms of wear exist [5–7]. Current applications of WC–Co coatings are on compressor piston rods, pump plungers, shaft sleeves on centrifugal pumps and fans and midspans of compressor blades in gas turbines.

Thermal sprayed coatings have residual stresses that can promote cracking of the coatings, leading, in this way, to a decrease in service lifetime. Residual stresses can arise from the following contributory factors: quenching stresses generated during the solidification of the splats, stresses generated during deposition by one pass of the gun, stresses generated while the sprayed specimen cools down after spraying (cooling stresses) and phase transformation stresses [8]. The residual stress distribution may be complex, and either tensile or compressive stresses may result at the surface of the coating. Tensile stresses are very detrimental for coating lifetime because these stresses tend to aid opening and propagation of the cracks. On the other hand, compressive stresses tend to close the cracks formed, enhancing the fatigue life of coatings. Compressive stresses in WC–Co coatings are produced by a 'peening' action of WC particles [9]. When unmelted or partially melted particles, such as WC, impact and plastically deform the substrate or coating, the 'peening' effect induces compressive stresses at the surface of the substrate and in subsequent layers of the coating. Various methods are available to quantify residual stresses such as drilling holes, X-ray diffraction or the Almen test [10–12] but the application of these techniques to complex coatings is difficult.

Acoustic emission (AE) has been used to predict failure processes [13] and monitor damage in loaded structures. AE is a term describing a class of phenomena whereby transient elastic waves are generated by a rapid release of energy from localised sources within a material. Three main types of AE data analysis have been carried out, namely AE activity analysis, AE parameter analysis and AE frequency analysis. AE activity analysis measures the amount of AE signals produced by a specimen and primarily gives information about the initiation and evolution of damage during a test. AE parameter analysis uses signal parameters such as ring down counts, amplitude energy and duration [14,15]. This type of analysis is useful for evaluating the severity of damage or for discriminating between different damage types. AE frequency analysis uses Fast Fourier Transform or wavelet analysis to calculate the frequency spectrum of the AE waves. This approach has been found useful in discriminating between damage mechanisms [16,17].

Thermal sprayed coatings have a very complex microstructure. Microcracking and macrocracking, as well as other processes, can release energy that can be monitored using AE technology. This technique combined with three- or four-point bend tests or tensile tests is very useful in generating data that allow the failure mechanisms of coatings to be understood better [18,19]. Studies carried out on thermal sprayed coatings indicate that the main failure processes are segmentation and delamination. Segmentation is defined as a network of cracks starting from the top surface of the coating that propagate in a direction perpendicular to it [20]. Delamination involves initiation and growth of cracks at the substrate–coating interface.

The applied stress at which these cracking mechanisms occur will be influenced by the magnitude of the residual stresses present in the coating. Hence, the aim of the present work is to investigate the failure mechanisms and residual stresses present in WC–Co coatings produced under various experimental conditions with different thermal spraying guns by subjecting samples to four-point bend tests using AE and scanning electron microscopy (SEM) to assess the damage. AE is used to detect the onset of coating damage and this is related to the magnitude of residual stresses present. SEM is employed to determine the nature of that damage. As information on the initiation of damage was required AE activity analysis was chosen as the principal technique to analyse the AE data.

2. Experimental procedure

A WC-12%Co powder, with a mean particle size of 35 μm, was used for spraying. Spraying was carried out in the CPT of the University of Barcelona. The substrate was an ASTM 1015 (mild steel) 150 mm in length, 25 mm in width and 3 mm in thickness (Fig. 1). It is reported that yield strength of this steel is 284 MPa [21]. Two different guns were utilised for spraying, a CDS

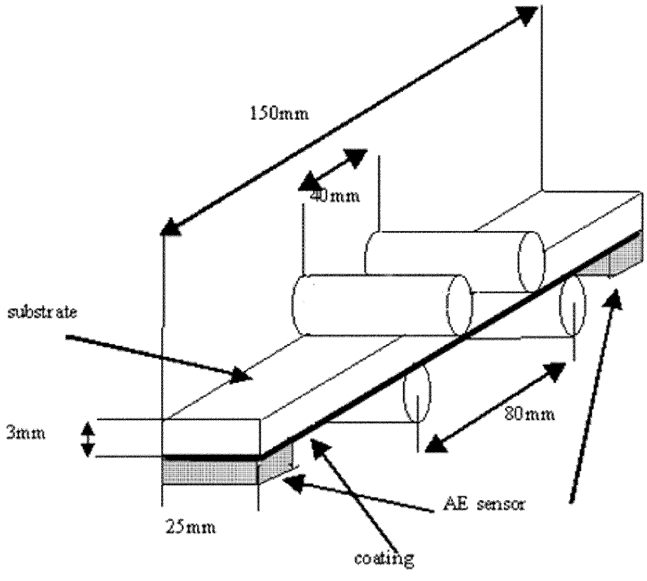

Fig. 1. Schematic diagram of the four-point bend test device. Coatings are tested under tensile stress.

Table 1
Spraying conditions for the samples tested

Sample	HVOF gun	O_2 (l min^{-1})	C_3H_6 (l min^{-1})	Spraying distance (μm)	Thickness (μm)	Vickers hardness, 300 g
A	DJ	253	77	300	300	1051±149
B	CDS	420	55	300	240	879±174
C	CDS	420	55	300	350	1020±99
D	CDS	420	55	250	90	1032±112
E	CDS	420	55	350	90	958±166

The DJ 2700 gun uses in addition 375 l min^{-1} of air.

100 (second-generation HVOF gun) and a DJ 2700 (third generation HVOF gun) (Sulzer Metco, Westbury, NY 11590). The spraying conditions and characteristics of the coatings are shown in Table 1. The DJ 2700 HVOF gun uses in addition 375 l min^{-1} of air.

For the AE measurements, the sample was tested in four point bending using an Instron tensile testing machine (100 Royal Street Canton, MA 02021–1089) operating at a fixed cross-head displacement rate. The coating was loaded so that it was subjected to tensile stresses. The inner and outer spans of the four-point bend device were 40 and 80 mm respectively. The cross-head speed was 0.5 mm min^{-1} (0.0083 mm s^{-1}) and the total test time was 720 s. Load and displacement were recorded for each test. Vallen AE-Suite (Schaeftlarner Weg 26, 82057 Icking, Germany) equipment with a preamplification of 34 dB was used to record the AE. The threshold value in AE measurements was set at 40 dB. By using two sensors this technique allowed the localisation of events as a function of distance from the sensors. A total of 3 samples were tested for each condition.

After testing, the surface of the samples was studied by SEM (SEM JEOL JSM-5310 1-2 Musashino 3-chome Akishima, Tokyo, Japan). Transverse sections were obtained by electric discharge machining followed by standard metallographic preparation procedures. These sections were examined by SEM in order to observe cracks resulting from loading the coating under tension.

3. Results and discussion

3.1. AE analysis of and correlation with cracking processes

The elastic modulus of the steel substrate is approximately 205 GPa. The elastic modulus of the coating designated 'A' was determined by a microindentation method [22] as 230 GPa. It can therefore be assumed that the coatings deform elastically during the elastic deformation of the substrate as the yield strength of the mild steel is relatively low.

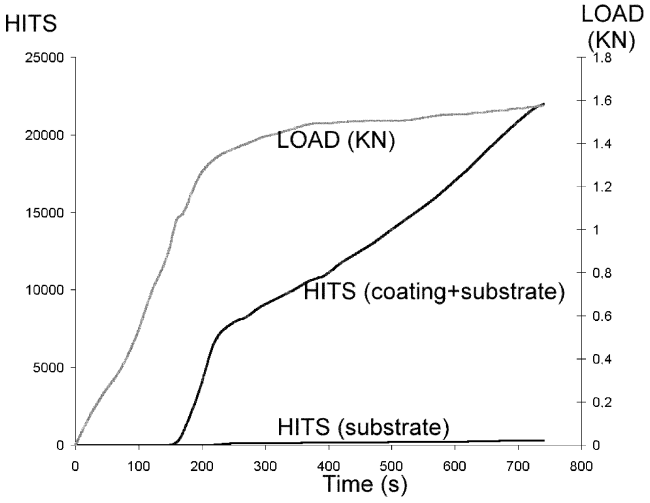

Fig. 2. Load applied and accumulative AE (number of hits) produced during the complete test (sample 'E3'). Two different AE regions are shown designated mild AE and severe AE.

Fig. 2 shows the load applied and the AE (accumulative number of hits) produced in sample 'E' (coating and substrate) as a function of time during a test in which the cross-head displacement rate is constant. A hit is defined as a signal that crosses the threshold amplitude. A pronounced change in gradient of the load versus time trace is observed at a loading time of 190 s corresponding to the onset of plastic deformation of the substrate. Two different regions with respect to the number of AE events observed are shown. The first one takes place at an initial period of 140 s of loading where a very low number of hits are produced, whereas a much greater number of AE hits arise after longer loading times corresponding to larger deformations. These two regions have been designated as mild AE and severe AE respectively.

Three samples from the 'E' group (Table 1) were subjected to different levels of deformation so as to relate the diverse cracking processes occurring to the AE signals registered during the four-point bend tests. To differentiate between the number of AE events in each test, the AE, defined as the number of accumulative hits received with respect to the time of testing in seconds, was determined.

Sample 'E1' was loaded for a time of 140 s corresponding to an elastic deformation of the coating and the substrate, sample 'E2' for a time of 190 s which corresponded to just before the onset of plastic deformation of the substrate and sample 'E3' for a time of 720 s. This corresponded to loading so as to produce plastic deformation of the substrate.

Microscopic observation of sample 'E1' revealed a lack of cracking in both the coating and at the substrate interface. A low AE rate of approximately 6 hits per second with a maximum amplitude of 60–65 dB was detected. The position where the AE events took place was analysed and found to be mainly at the contact points of rollers of the four-point bend device. Thus, friction processes between the coating and rollers are thought to be responsible for the AE signals generated in sample 'E1'.

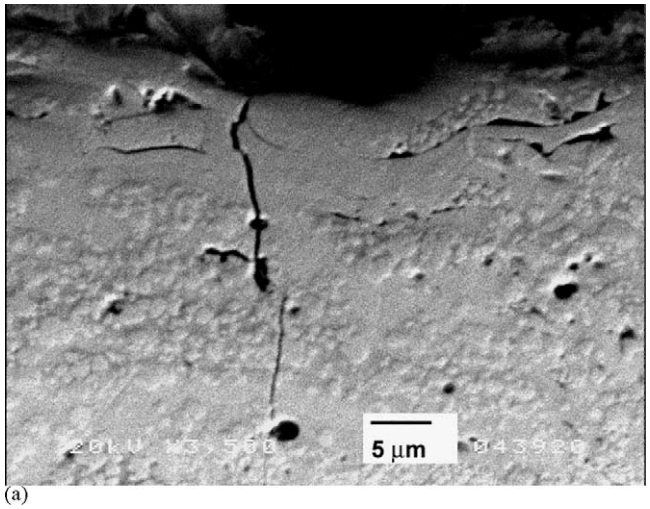

(a)

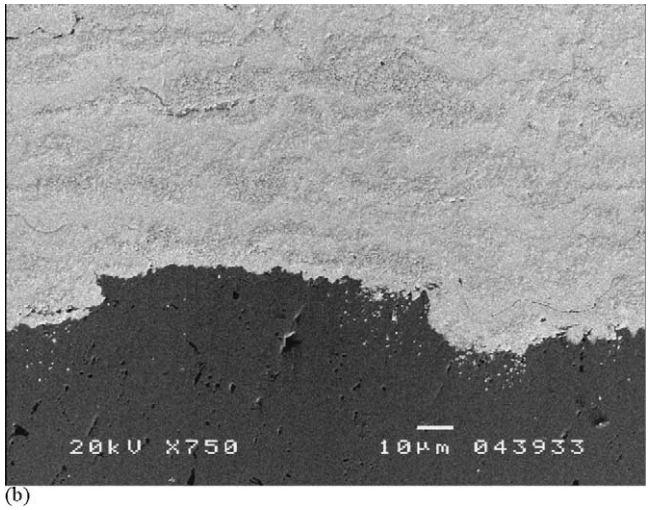

(b)

Fig. 3. (a) Narrow crack observed in sample 'E2'. In all cases cracks do not reach the substrate. (b) Substrate–coating interface in sample 'E2'. Note that the substrate/coating interface remains intact and does not exhibit cracks or voids.

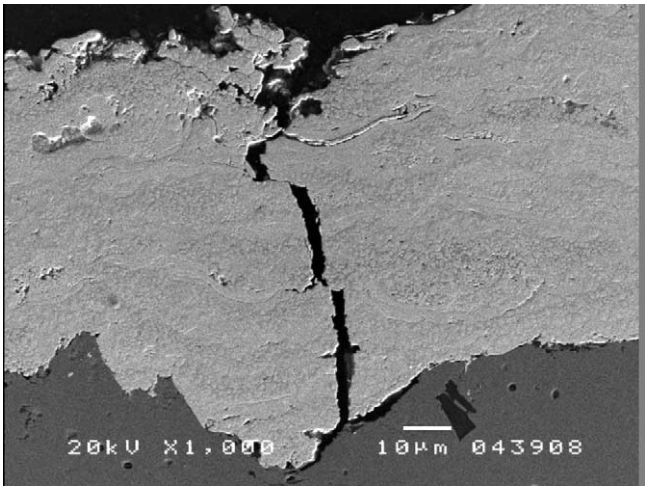

Fig. 4. Damaged interface in sample 'E3'. Once the crack has reached the interface cracks propagate along it leading to delamination.

A metallographically-prepared cross-section of sample 'E2' showed the existence of cracks propagating perpendicular to the coating surface (Fig. 3). Cracks, which are very narrow, i.e. with a small crack tip opening displacement, do not reach the substrate in all cases and the interface does not reveal any debonded areas (Fig. 4). Microscopic observation of the free surface of the coating did not reveal the presence of cracks, indicating that their thickness was not sufficient to allow them to be detected on the rough surface of the coating. The rate of AE in this sample, approximately 100 hits per second, was much greater than that in sample E1. The maximum amplitude of hits was 85–90 dB, which was greater than that observed in sample 'E1'.

A cross-section of sample 'E3' revealed a large number of cracks, all of which reached the substrate. Once they reached the substrate, they propagated along the interface between the substrate and the coating as

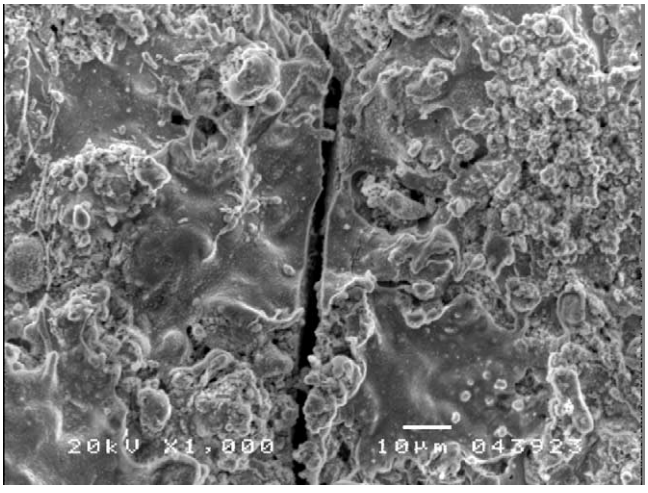

Fig. 5. Damaged surface in sample 'E3'. Note the straight nature of the crack. This crack extended across the complete width of the sample, 25 mm.

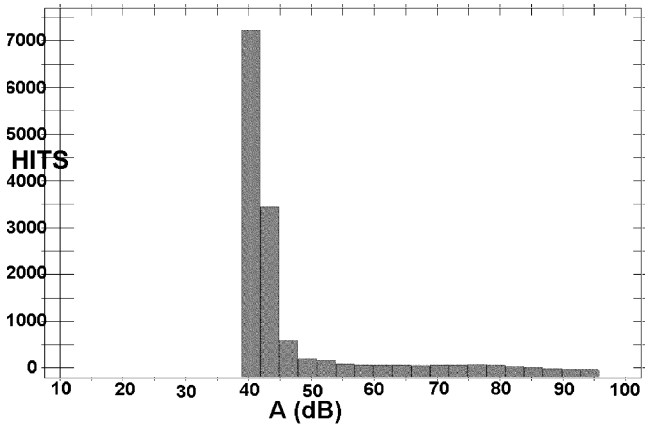

Fig. 6. Accumulative number of hits as a function of amplitude for sample 'E3'. Note the high amplitude hits that in some cases reach 95 dB.

can be seen in Fig. 5. The rest of the interface was unaltered. The surface of the coating showed cracks with a width of approximately 5 μm (Fig. 6). These cracks were present in greater number between the inner rollers but some were also present between the external and internal rollers. The rate of AE was high, of the same order of magnitude as that in sample 'E2'. Cracking produced during testing seems to be related to the AE recorded because in the samples where cracks appeared a greater AE activity was detected (case of samples 'E2' and 'E3'). The maximum amplitude of hits was approximately 95 dB (Fig. 7).

A microscopic analysis of the crack morphology in sample 'E3' was performed. It was found that cracks propagate perpendicular to the coating surface, but in some cases crack branching was observed. Cracks tend to grow easily in areas where more dissolution of WC has occurred because of the poorer properties of this region [6]. Dissolution of WC takes place during

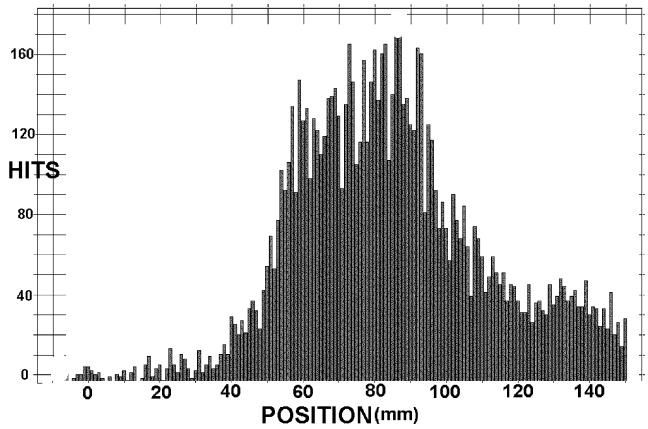

Fig. 7. AE signal as a function of distance along the sample 'E3'. Note that the AE signals are mainly located between the two inner rollers at 55 and 95 mm.

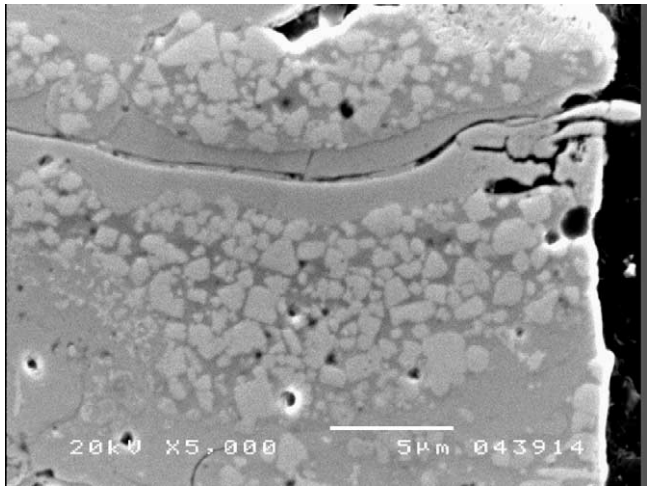

Fig. 8. Preferential cracking in a WC degraded area due to its inferior fracture toughness.

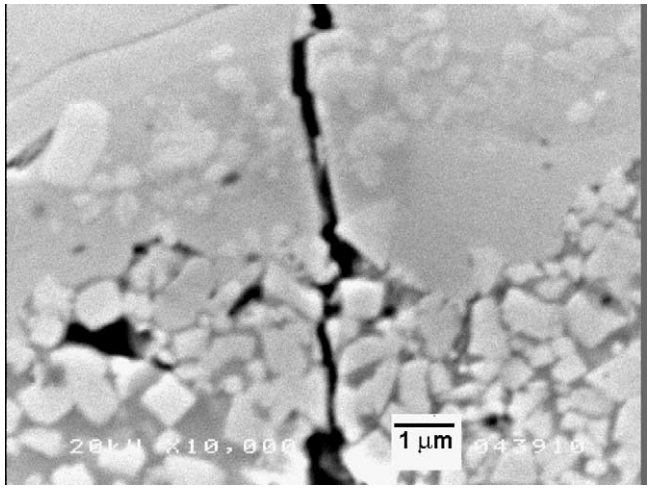

Fig. 9. Detailed nature of crack path. Note that the cracks tend to propagate at the Cobalt–WC interface.

spraying due to the elevated temperature of the spraying flame. WC is totally degraded in some areas. Fig. 8 shows preferential cracking in an area of WC dissolution. Higher magnification reveals that the crack propagates along the interface between WC and cobalt (Fig. 9). Some cracks are formed from smaller cracks with different growth directions and appear as distinct steps apparently produced at different stress levels during testing, but other cracks are straight, totally perpendicular to the substrate surface (Figs. 10 and 11).

Fig. 12 presents a schematic of the cracking mechanism occurring during the four-point bend test. Four different regions are distinguished: Region 1: at short times corresponding to small displacements and surface stresses no cracks are formed. Region 2: this region is still situated in the elastic stress regime of the substrate. Initiation and discontinuous propagation of cracks begins. Region 3: this region is located after the onset

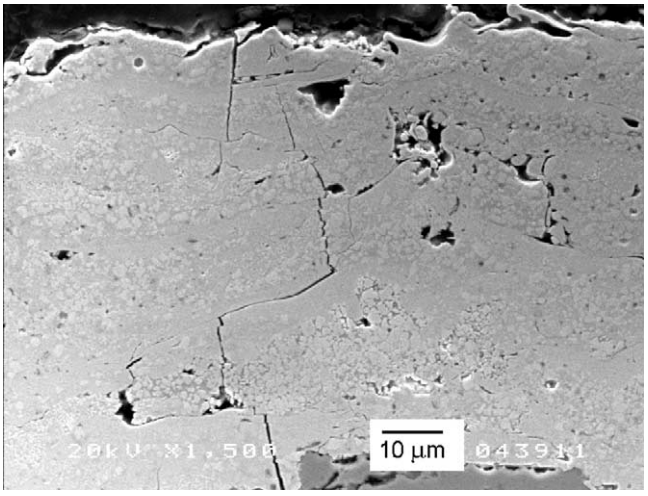

Fig. 10. Stepped nature of the cracks found in sample'E3'. These steps are thought to arise at different times during the test.

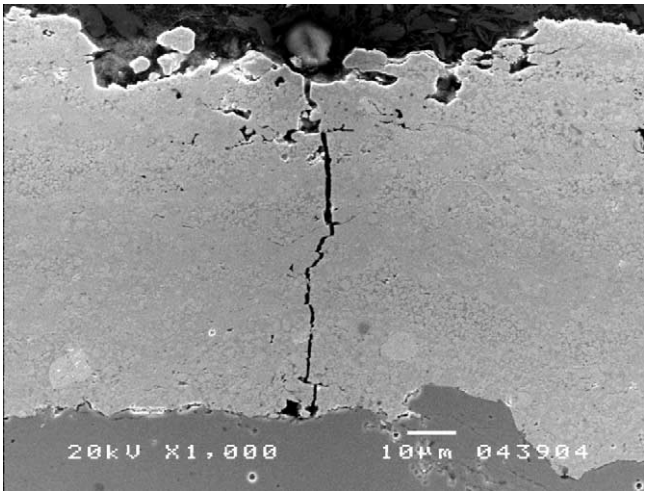

Fig. 11. Sample 'E3' showing a crack propagating in a straight, nonstepped manner to the substrate indicating that it was probably produced as one event. Note the delamination at the substrate–coating interface.

of plastic deformation of the substrate. The coating cannot deform plastically and rapid crack propagation is produced due to the low fracture toughness of the coating. It is reported that the fracture toughness of thermally sprayed WC–Co determined by microindentation using the Lawn and Fuller equation varies from 2 to 4 Mpa $m^{\frac{1}{2}}$ depending on the initial powder used for spraying [23]. The fracture toughness of the coatings parallel and transverse to the substrate is also different [24]. Cracks reach the substrate in all cases. Region 4: after the cracks reach the substrate, they propagate along the interface between the substrate and the coating causing delamination.

Fig. 13 shows the amplitude of AE signals during the complete test, i.e. during the four regions referred to above. Low amplitude signals are produced in region 1, mainly provoked by friction between the coating and rollers applying the load. This region also shows a low rate of AE activity (mild AE). Region 2 has high amplitude signals below 85 dB that correlate with the initiation and discontinuous propagation of cracks. In this region severe AE starts indicating that cracking produces a large number of hits.

The highest amplitude signals (95 dB) are produced in region 3. These signals correlated with the rapid crack propagation that takes place in the WC–Co coating during plastic deformation of the substrate. The maximum amplitude of hits in region 4 is less than that in region 3, being <80–85 dB. Thus, delamination processes produce lower amplitude events than crack growth through the coating.

A test carried out on the substrate free of coating indicates that the AE produced during its plastic deformation is almost negligible compared to the AE produced by the coating.

3.2. Analysis of the residual stresses in the WC–Co coatings

The presence of tensile residual stresses may produce cracking of coatings at surface stresses and deformation corresponding to shorter times of testing at a fixed cross-head displacement rate. AE allows the start of the cracking processes to be quantified as the onset of severe AE, which corresponds to the initiation and propagation of cracks. For this reason, the start of severe AE was used as the parameter to rank the cracking resistance and residual stress present in the coatings.

The expression $\sigma = 3Fd/(bh^2)$ can be used to calculate the stress at the surface of a coating loaded in symmetric four point bending provided that the deformation remains elastic [25]. In the above expression F is the force, d the distance between the inner and outer rollers, b the sample width and h the sample thickness. Table 2 show the stress where severe AE begins. The differences presented in Table 2 are not a result of different intrinsic properties of the coatings because all the coatings have a similar structure, phases distribution and hardness values (Table 1). Higher surface roughness could produce easier crack initiation but the roughness parameters of all samples were similar. In the case of sample B, $R_a = 5.1$ µm, $R_t = 33$ µm, whereas for sample D, $R_a = 4.9$ µm, $R_t = 35$ µm. R_a is the standard deviation with respect to the mean value whereas R_t is the maximum peak to valley distance. Samples B and D start severe AE at very different stresses. This can only be related to different residual stresses present in the coating because these coatings are identical except for their thickness.

To calculate the stress when crack starts it was assumed that the total thickness of the samples (coating+substrate) was identical in all cases because the

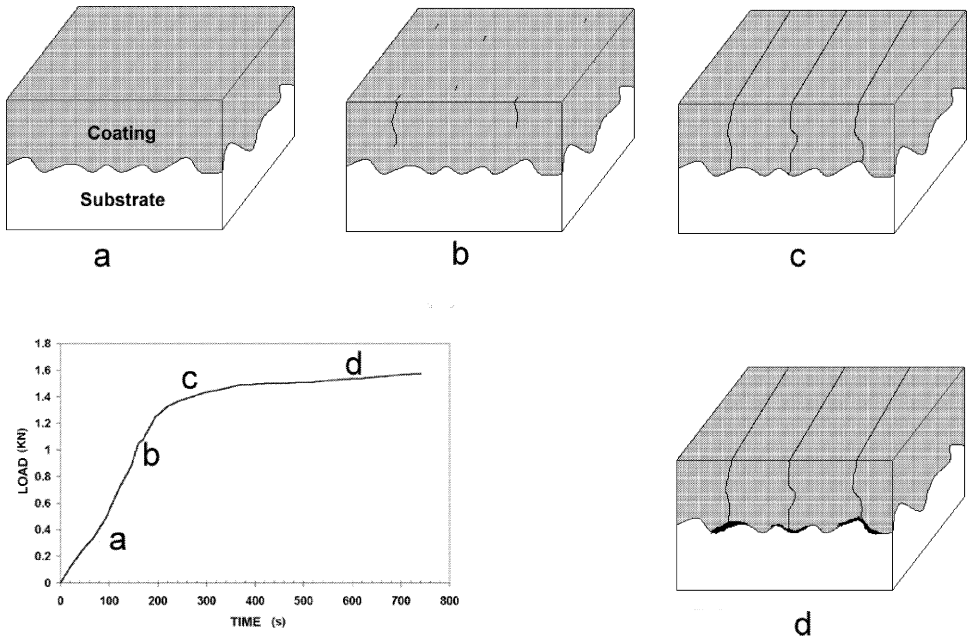

Fig. 12. A schematic representation of the cracking processes occurring during the four-point bend tests on WC–Co coatings.

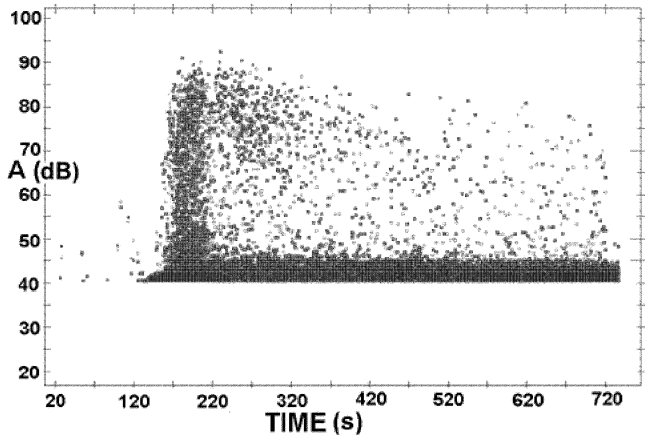

Fig. 13. Amplitude of hits as a function of time during the test. Note the variation of the maximum hit amplitude during the test.

contribution of slightly different coating thickness to the total sample thickness is almost negligible.

The stress acting on materials that contain residual stresses is given by the expression:

$$\sigma_t = \sigma_i + \sigma_s \quad (1)$$

where σ_t is total stress on the coating, σ_i is the applied stress on the coating produced from an external known load and σ_s is the residual stress on the coating. If the coating strength is defined as the critical value of stress, σ_t, at which severe AE starts the relative cracking resistance and levels of residual stresses present in the coatings produced under different spraying conditions can be elucidated from measurements of σ_i. Coatings with high values of σ_i will have lower tensile residual stresses or negative (compressive) residual stresses present at the surface. If samples 'A' and 'C', which have similar coating thickness, are compared it can be seen that the cracking resistance of coatings obtained with the DJ 2700 gun is higher than that obtained with the CDS 100 gun. This indicates that the DJ 2700 gun produced lower tensile residual stresses in the WC–Co coatings (Table 2). The higher velocity particles achieved by the DJ 2700 gun could promote the shot peening effect of the WC enhancing the compressive residual stresses in the coating and so increasing the stress at which cracking starts.

Table 2 indicates that spraying distances from 250 to 350 mm have very little effect on the cracking resistance if the coating thickness is maintained constant. When the spraying distance is varied residual stresses may be

Table 2
The stress (σ_i) at which severe AE occurs

Gun		Spray distance (mm)		Thickness (μm)		
CDS 100 (C)	DJ 2700 (A)	250 (D)	350 (E)	90 (D, E)	240 (B)	350 (C)
110±10 MPa	154±13 MPa	193±9 MPa	194±8 MPa	193 MPa	119±11 MPa	110±10 MPa

This can be taken as a measure of cracking resistance. The name of the samples is between brackets.

influenced by three factors. The shot peening effect produces a lower compressive residual stress effect when the spraying distance is greater due to the lower impact velocity of the powder particles when they impact the substrate. At the same time the residual stresses from quenching the semi molten impacted particle (always tensile) and from cooling the deposited coating and substrate (compressive in our case) are modified by spraying distance as this affects the substrate temperature. In the present case it would appear that these three factors combine to result in little change to the residual stresses present as a function of spraying distance.

The effect of the coating thickness is very important. Higher coating thickness, for constant spraying parameters, give lower cracking resistance. Included in Table 2 is the theoretical value of crack resistance for a 90-μm thick coating. This value is obtained from the mean value of cracking resistance for coatings D and E sprayed with a spraying distance of 350 and 250 mm as spraying distance has been shown to have little effect on cracking resistance. Increase in the number of layers deposited tends to increase the temperature of the substrate/coating and thus modify the residual stresses present. Some authors indicate that the optimum substrate temperature depends on the relative thickness of the coating [26]. In the present system it seems that to increase the cracking resistance of the coating (i.e. reduce the tensile residual stresses or improve the compressive stresses) the optimum coating thickness is 90 μm.

4. Conclusions

(1) Two different regions of AE are observed. The first region, which has a low rate of AE, finishes when cracking processes appear. Cracking in coatings produces a high rate of AE and the stress at which this occurs is a useful parameter in assessing cracking resistance.

(2) WC–Co coatings show, during four-point bend testing, different cracking processes. After initiation, discontinuous crack propagation takes place until plastic deformation of the substrate occurs at which point crack propagation is rapid. After cracks reach the substrate they propagate along the substrate–coating interface producing delamination. The maximum amplitude of hits depends on the cracking process. Thus, crack initiation and propagation produces a maximum hit amplitude of approximately 95 dB, whereas the maximum hit amplitude for delamination is 80–85 dB.

(3) Crack propagation in degraded WC areas is very easy because of its inferior fracture toughness. Preferential crack propagation along the Cobalt–WC interface is also shown in non-degraded areas.

(4) Residual stresses depend on the HVOF gun used and the coating thickness. Thus, a higher cracking resistance and lower tensile residual stresses are found for lower thickness coatings. The use of the DJ 2700 gun instead of the CDS 100 gun also improves cracking resistance. No significant differences in cracking resistance are observed as a function of spraying distance.

Acknowledgements

This work was performed with the support of the Generalitat de Catalunya (1999SGR00051). J.M. Miguel wishes to give special thanks to the University of Barcelona for the concession of this award. Special thanks to M. Browne and A. Roques of the Bioengineering Group of the University of Southampton for their advice with the A.E. work as well as to C. Lorenzana for his help.

References

[1] H. Herman, S. Sampath, in: K.H. Stern (Ed.), Metallurgical and Ceramic Protective Coatings, Chapman&Hall, London, UK, 1996, pp. 261–289.
[2] J.M. Guilemany, J.A. Calero, Soldadura y Tecnologías de Unión 55 (1999) 9–15.
[3] H. Kreye, S. Zimmermann, P. Heinrich, in: Akira Ohmori (Ed.), Proceedings of ITSC'95, Japan, 1995, pp. 393–398.
[4] J.M. Guilemany, J.M. de Paco, J. Nutting, J.R. Miguel, Metall. Mater. Trans. A 30 (1999) 1913–1921.
[5] V. Fervel, B. Normand, H. Liao, C. Coddet, E. Beche, R. Berjoan, Surf. Coat. Tech. 111 (1999) 255–262.
[6] L. Jacobs, M. Hyland, M. De Bonte, J. Therm. Spray Technol. 8 (1) (1999) 125–133.
[7] J.M. Guilemany, J.M. de Paco, in: T.S. Sudarshan, M. Jeandin, K.A. Khor (Eds.), Surface Modification Technologies XI (Paris, France, 1997), IOM Ltd, London, UK, 1998, pp. 982–990.
[8] Lech Pawlowski, The Science and Engineering of Thermal Spray Coatings, Wiley, Chishester, England, 1995.
[9] J.J. Han, R. Knight, L.S. Schadler, in: E. Lugscheider, P.A. Kammer (Eds.), United Thermal Spray Conference, (Düsseldolf, Germany, 1999), DVS, 1999, pp. 771–776.
[10] X. Provot, H. Burlet, M. Vardavoulias, M. Jeandin, D. Manesse, C. Richard, J. Lu, in: C.C. Berndt (Ed.), Proceedings of the 1993 National Spray Conference, (Anaheim, CA, 1993), ASM International, 1993, pp. 159–165.
[11] O. Bradt, in: Akira Ohmori (Ed.), Proceedings of ITSC'95, Japan, 1995, pp. 639–643.
[12] R. Knight, R.W. Smith, in: C.C. Berndt (Ed.), Proceedings of the 1993 National Spray Conference, ASM International, USA, 1993, pp. 607–612.
[13] A.G. Evans, M. Linzer, J. Am. Ceram. Soc. 56 (11) (1973) 575–581.
[14] C. Lin, C.C. Berndt, S. Leigh, K. Murakami, J. Am. Ceram. Soc. 80 (9) (1997) 2382–2394.
[15] J. Voyer, F. Gitzhofer, M.I. Boulos, J. Therm. Spray Technol. 7 (2) (1998) 181–190.
[16] G.N. Morscher, J.Z. Gyekenyesi, Ceram. Eng. Sci. Ads 19 (1998) 241–249.

[17] J. Martínez-Fernández, G.N. Morscher, J. Eur. Ceram. Soc. 20 (2000) 2627–2636.
[18] K. Akita, G. Zhang, S. Takahashi, H. Misawa, S. Tobein, in: C. Coddet (Ed.), Proceedings of the 15th International Thermal Spray Conference, ASM International, France, pp. 837–842.
[19] J. Voyer, F. Gtzhofer, M.I. Boulos, J. Dionne, in: C.C. Berndt (Ed.), Thermal Spray: Practical Solutions for Engineering Problems, ASM International, Ohio, USA, 1996, pp. 303–310.
[20] F. Bordeax, C. Moreau, R.G. Saint Jacques, Surf. Coat. Technol. 54/55 (1992) 70–76.
[21] Mechanical Properties of Carbon and Alloy Steels,J.R. Davis (Ed.), Metals Handbook, Desk Edition, ASM International, Ohio, USA, 1998, pp. 219–225.
[22] D.B. Marshall, T. Noma, A.G. Evans, Comunications Am. Ceram. Soc. (1982) 175–176.
[23] S.de Palo, M. Mohanty, H. Marc-Charles, M. Dorfmanin, in: C.C. Berndt (Ed.), Thermal Spray Surface Engineering via Applied Research, ASM International, Canada, 2000, pp. 245–250.
[24] E. Lopez Cantera, B.G. Mellor, Materials Lett. 37 (4–5) (1998) 201–210.
[25] G. Gualco, S. Corcorutu, A. Campora, R. Taylor, D. Schwingel, S. Orwald, in: C.C. Berndt (Ed.), Thermal Spray: A United Forum for Scientific and Technological Advances, ASM International, USA, 1997, pp. 305–313.
[26] S. Takeuchi, M. Ito, K. Takeda, Surf. Coat. Technol. 43/44 (1990) 426–435.